

**Investigation of the two-gap superconductivity in a few-layer NbSe<sub>2</sub>-graphene heterojunction**

Tianyi Han, Junying Shen, Noah F. Q. Yuan, Jiangxiazi Lin, Zefei Wu, Yingying Wu, Shuigang Xu, Liheng An, Gen Long, Yuanwei Wang, Rolf Lortz, and Ning Wang\*

*Department of Physics and Center for Quantum Materials, The Hong Kong University of Science and Technology, Hong Kong, China*

(Received 11 September 2017; revised manuscript received 3 February 2018; published 16 February 2018)

We investigated the superconductivity in a few-layer NbSe<sub>2</sub>-graphene heterojunction by differential conductance spectroscopy. Because of the gate-tunable Fermi level of the few-layer graphene, used here as a tunneling electrode in a nano-point-contact spectroscopy setup, the differential conductance of the heterojunction showed highly sensitive dependence on the gate voltage, which allowed us to probe the nature of the superconducting gap functions with unprecedented detail by continuously tuning the transparency of the junction between the spectroscopic tunneling and the Andreev reflection limits. Characteristic features associated with a two-gap superconductivity in NbSe<sub>2</sub> were reproducibly observed in both limits and between, e.g., in the form of a central conductance dip with two sets of coherence peaks when the Fermi level was close to the charge neutrality point of graphene. From fits with the Blonder-Tinkham-Klapwijk model, two gaps with their temperature dependence were extracted. The two gaps associated with the two-band superconductivity in NbSe<sub>2</sub> followed the expected temperature behavior in the limit of weak interband scattering, with a gap to  $T_c$  ratio suggesting a weak to moderately strong coupling in few-layer systems.

DOI: [10.1103/PhysRevB.97.060505](https://doi.org/10.1103/PhysRevB.97.060505)

Since the report on the realization of a single layer of graphite—the graphene—in 2004 [1], there is a rapid growth of research on various two-dimensional (2D) materials due to their unusual physical properties, which are of high fundamental and technological relevance. 2H-NbSe<sub>2</sub> as a layered transition-metal dichalcogenide is of particular interest as an intrinsically superconducting material with very unusual properties. It represents an ideal platform for the study of superconductivity from a bulk system to the extreme 2D limit. Previous studies have shown that the bulk NbSe<sub>2</sub> can be described as either a strongly anisotropic *s*-wave superconductor or a two-gap superconductor [2–7]. Recently, due to the maturity of the micromechanical exfoliation technique, superconductivity has been preserved in atomically thin NbSe<sub>2</sub>. This makes it possible to tune the charge-carrier concentration and thus to modulate the superconducting properties in a wide range via the electric field effect [8,9]. In addition, with the advantage of the protective hexagonal boron nitride (hBN) capping, superconducting NbSe<sub>2</sub> down to the monolayer limit was fabricated with high crystalline quality [10]. As an effect of the extremely large spin-orbit coupling in an inversion asymmetric transition-metal dichalcogenide monolayer, it was found that the upper critical field of mono- or few-layer NbSe<sub>2</sub> in magnetic fields applied parallel to the layers, largely exceeds the BCS Pauli limit for superconductivity due to a mechanism now called Ising superconductivity [10–14]. In addition, it was theoretically predicted that the Ising superconducting phase of monolayer NbSe<sub>2</sub> would be a nodal topological phase in which nodal points are connected by Majorana flatbands on the edge [15]. Specular Andreev reflection (AR) was studied both experimentally [16,17] and theoretically [18,19] in bulk

NbSe<sub>2</sub>-graphene heterojunctions. However, apart from the intriguing transport features, the investigation of the gap structure of atomically thin NbSe<sub>2</sub> and the superconductivity in van der Waals heterostructures composed of few-layer NbSe<sub>2</sub> remains elusive. In this work, we investigated superconductivity in a hBN-encapsulated few-layer NbSe<sub>2</sub>/graphene heterojunction by differential conductance spectroscopy, using graphene as a gate-tunable point-contact-like probe to obtain energy-resolved information about the superconducting gap structure of NbSe<sub>2</sub>. A strongly gate-dependent differential conductance was observed and two gaps together with their temperature dependence were extracted using fits with the Blonder-Tinkham-Klapwijk (BTK) model [20]. The unique possibility of tuning the barrier transparency continuously over the graphene gate allowed us to examine in detail the temperature dependence of the two superconducting gaps in the tunneling regime. The two-gap followed the temperature behavior of two-band superconductors with weak interband scattering.

The graphene-NbSe<sub>2</sub> junction was sandwiched by thin BN flakes using the well-established transfer method [21]. The lower BN layer was first prepared by exfoliation on a Si/300 nm SiO<sub>2</sub> wafer, and the few-layer graphene was dry transferred to the BN, followed by a wet transfer of a few-layer NbSe<sub>2</sub>. Electron-beam lithography was followed by fabrication of 10 nm/50 nm Ti/Au terminals to both the graphene and NbSe<sub>2</sub> layers. After the liftoff, another thin BN was capped onto the junction.

Both ac and dc+ac methods were used to study the transport behavior of the junction in a 2 K base temperature cryostat. For the ac measurement, a Stanford Research DS360 low-distortion function generator was used as a voltage source in combination with a Stanford Research SR830 and a Signal Recovery 7280 wide-bandwidth digital lock-in amplifier, which were used to measure the voltage and current signals

\*phwang@ust.hk

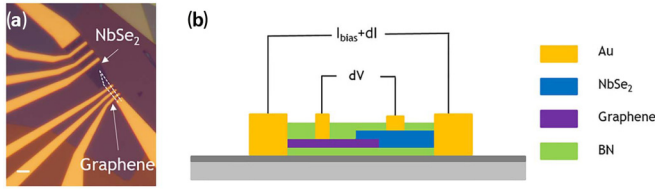


FIG. 1. Structure of the NbSe<sub>2</sub>-graphene heterojunction. (a) Optical images of the heterostructure before top BN capping. (b) Sketch of the device structure and the measurement setup for differential conductance measurement. Scale bar: 3  $\mu\text{m}$ .

at a low frequency, respectively. Gate voltages were applied with an Aim-TTi International PLH120 dc power supply. For the differential conductance spectroscopy, a Keithley 6221 ac and dc current source was used to apply a dc current bias with small ac current modulation to the outer two probes across the junction. An SR830 lock-in amplifier was used to measure the ac response across the junction on the inner two probes at a frequency of 771 Hz. A sketch of the measurement setup is shown in Fig. 1(b). The bias voltage across the graphene/NbSe<sub>2</sub> junction was extracted by integrating the differential resistance versus the bias current, and subtracting the voltage drop on graphene channel resistance in between the two voltage terminals (discussed in detail in the Supplemental Material [22]).

Both the pristine few-layer NbSe<sub>2</sub> and the few-layer graphene were first characterized by standard ac transport measurements. The NbSe<sub>2</sub> layer showed an onset  $T_c \sim 4$  K and out-of-plane upper critical field  $B_{c2} \sim 2$  T. The charge neutrality point (CNP) of pristine few-layer graphene was located at  $V_g = -3.4$  V, as denoted by the resistance maxima. For the NbSe<sub>2</sub>/graphene heterojunction, the CNP shifted to  $V_g = -4.2$  V. Differential conductance against bias voltage was measured across the heterojunction, as shown in Fig. 2.

Figure 2(a) shows the differential conductance spectra at 2 K, which show nonlinearity at different gate voltages and sensitive dependence on the gate voltage. When we tuned the Fermi level to near the CNP of the junction, the conductance showed a central dip with two sets of coherence peaks, as denoted by the light-blue data. The inner set of coherence peaks

was located at  $I_{\text{bias}} \sim \pm 1.5 \mu\text{A}$ , while the outer set occurred at around  $\pm 3.5 \mu\text{A}$ . Since the Fermi level was continuously tuned away from the CNP, the central conductance dip with the inner set of coherence peaks were gradually suppressed and evolved into a broad conductance peak, which emerged at zero bias current with gate voltage at  $-3.8$  and  $-4.8$  V, to a well-formed peak at  $-3.5$  and  $-5.0$  V, respectively. The outer set of coherence peaks hardly changed as indicated by the dark blue and red data in the figure.

Figure 2(b) provides a complementary illustration of the gate-dependent differential conductance. The data value in the figure is the differential conductance at 2 K normalized by the 5 K value above the  $T_c$  of NbSe<sub>2</sub>. In the figure, the central blue oval area denotes the conductance dip at the CNP, while the red areas above and below correspond to the broad conductance peak. The two light stripes at the edges represent the outer set of coherence peaks.

The gate-tunable differential conductance is a manifestation of the variable interface transparency  $Z$ , which is tuned by the carrier density in graphene. When the Fermi level was close to the CNP, the relative contact resistance at the NbSe<sub>2</sub>/graphene interface is high, resulting in a single-particle tunneling behavior for the carriers injected across the junction [23,24]. Thus, a central dip was present, with the coherence peaks indicating roughly the superconducting gap values. On the other hand, when away from the CNP, the carrier density in graphene steadily increased, hence the interface became more transparent with reduced contact resistance. In this case, graphene functioned as a normal-metal lead, resulting in a gate-voltage-induced crossover from the tunneling limit to the Andreev limit, causing the broad central conductance peak [25]. This interplay of tunneling and AR tuned by electrical gating is unique in a superconductor/graphene interface, thanks to the gate-tunable carrier density of the semimetallic graphene [1,26].

The standard BTK model [20] describes both the high-barrier tunneling limit and the low-barrier Andreev regime, and in between, at a junction between a normal-metal electrode and a superconductor. For a monolayer graphene electrode, the BTK model needs to be modified to account for its unique specular Andreev reflections and the linear band structure [17,27]. However, these effects are absent in our junction with a few-layer graphene electrode. Specular reflections can be suppressed in the latter by the large potential barrier we have at the interface [19]. Moreover, the effect from the energy dependence of the density of states on the BTK fits is weakened when the thickness of graphene increases from monolayer to few layer, which mimics the characteristics of a normal metallic electrode. The standard BTK model thus allows us to reliably extract the superconducting gap values of NbSe<sub>2</sub>. Indeed the signature of specular Andreev reflection is completely absent in our mapping plot Fig. 2(b) and thus we use the standard two-gap BTK model for normal-metal/superconductor junction for the analysis of our results of the few-layer graphene/NbSe<sub>2</sub> heterostructure. In Fig. 3 we show the temperature dependence of the differential conductance of the heterojunction at two gate voltages in the tunneling limit together with the BTK fits. It is obvious that the nonlinear differential conductance spectra gradually lose their pronounced characteristics with increasing temperature due to the presence of superconductivity. The temperature scale

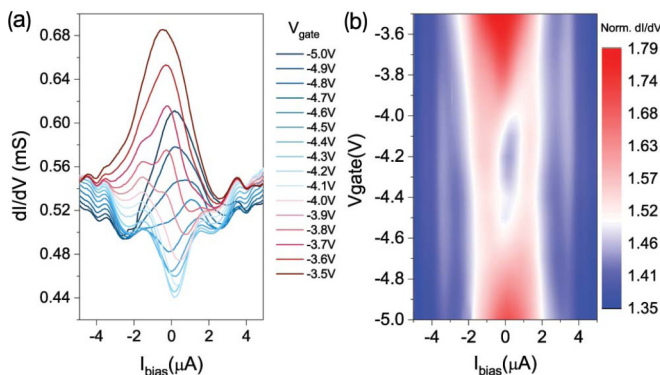


FIG. 2. Gate dependency of the differential conductance of the NbSe<sub>2</sub>-graphene junction. (a) Differential conductance of the junction at various gate voltages at 2 K. (b) Mapping of the normalized differential conductance versus gate voltage and bias voltage.

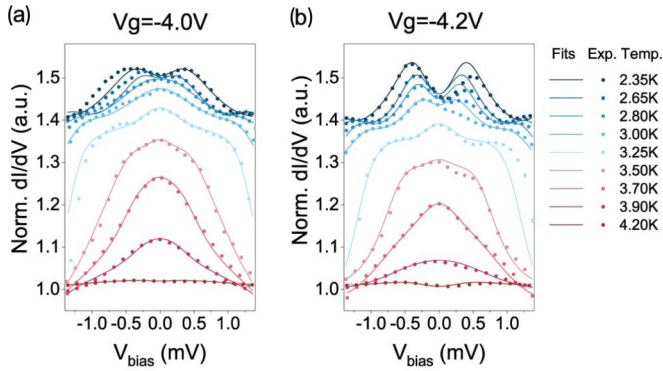


FIG. 3. Temperature dependence and BTK fitting of the normalized differential conductance of the graphene-NbSe<sub>2</sub> junction. Gate voltage: (a)  $-4.0$  V, (b)  $-4.2$  V. The lines are the fitting curves, and the dots are the experimental raw data at various temperatures normalized by the data at 5 K.

for the nonlinearity is consistent with the  $T_c$  of pristine NbSe<sub>2</sub> of the junction for all three gate voltages. We further carry out the fits for the differential conductance in the Andreev regime, and the  $Z$  values for distinct gate voltages acquired from the BTK fitting fully agree with our analysis of the gate-tunable interface transparency. If  $V_g = -4.9$  V, the junction was transparent and  $Z = 0.05$ – $0.2$ . When  $V_g$  was close to  $-4.2$  V,  $Z$  increased to 0.6, indicating a higher barrier at the interface.

The BTK fitting of the two data groups in the tunneling limit yielded the temperature dependence of the two gaps as shown in Fig. 4. From the figure we can conclude that for two gate voltages the gap values and their temperature dependence follow a similar trend. The multiple sets of coherence peaks in the differential conductance spectroscopy correspond to the two gaps. We observe that for the temperature dependence, the smaller gap differs significantly from the conventional BCS

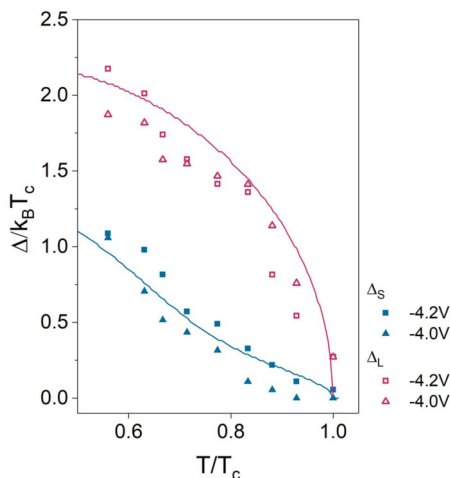


FIG. 4. Temperature dependence of the superconducting gap values extracted from BTK fits. Open symbols correspond to the larger gap, and solid symbols correspond to the smaller gap. The triangles and squares denote different gate voltages, respectively, as indicated in the legend. The two solid lines are fits of the two gaps using two-band BCS theory with small interband scattering. The ratio of interband scattering to intraband interaction is  $7 \times 10^{-3}$ .

tendency [28], which provides a temperature dependence that saturates at low temperature and closes abruptly at the critical temperature. However, the small gap here does not suddenly disappear at  $T_c$ , but has a pronounced tail feature when the temperature approaches  $T_c$ . This temperature dependence actually follows the expected behavior of a two-band superconductor with small interband scattering, as theoretically described by Suhl *et al.* [29] and experimentally verified in bulk NbSe<sub>2</sub> by Rodrigo and Vieira [2]. Since bulk NbSe<sub>2</sub> was previously shown to be a two-band superconductor, it is reasonable to assign the two gaps to a two-band nature of superconductivity in few-layer NbSe<sub>2</sub>. In the bulk NbSe<sub>2</sub>, from both electrical transport and specific-heat data [2–4],  $\Delta_S \sim 0.7$  meV and  $\Delta_L \sim 1.4$  meV, with a gap to  $T_c$  value  $\Delta(0)/k_B T_c \sim 1.8$ – $1.95$ . For our few-layer NbSe<sub>2</sub> sample, the two gap sizes reduce to  $\Delta_S \sim 0.39$  meV and  $\Delta_L \sim 0.79$  meV.

To roughly estimate the interband scattering strength, we further use a two-band BCS model to fit the temperature dependence of the two gaps. As shown by the two solid lines in Fig. 4, the two-band model with weak interband scattering fits our data well with a ratio of interband scattering to intraband interaction of  $7 \times 10^{-3}$ . As to the reduced gap values in few-layer NbSe<sub>2</sub>, by considering the reduction of  $T_c$ , the fit provides  $\Delta_S(0)/k_B T_c = 1.40$  and  $\Delta_L(0)/k_B T_c = 2.25$ , respectively, suggesting a weak to moderately strong coupling strength for few-layer NbSe<sub>2</sub>. By comparing with the gap to  $T_c$  ratio of the bulk system, it might indicate an enhanced coupling in few-layer NbSe<sub>2</sub>. We should mention that the extraction of bias voltage may cause a deviation, where more accurate results of tunneling experiments and analysis with extended models for multiband superconductors [30] are expected.

In conclusion, we investigated the superconducting gap structure of a few-layer NbSe<sub>2</sub> sample by fabricating a hBN sandwiched NbSe<sub>2</sub>-graphene heterojunction, in which the graphene served as a gate-tunable electrode in a nano-point-contact spectroscopy configuration. The differential conductance showed a characteristic nonlinearity below the superconductivity critical temperature of NbSe<sub>2</sub>, and a sensitive dependence on the applied gate voltages. For the gate-tunable carrier density near the CNP of the junction, the conductance showed a central dip with two sets of coherence peaks due to the high potential barrier from the contact resistance when the carrier concentration in the graphene layer was relatively low. When the Fermi level was tuned away from the CNP, a pronounced conductance peak emerged around zero bias, indicating a relatively transparent interface in which graphene was basically a normal metallic lead. Fitting of the temperature-dependent conductance spectra with the BTK model yielded consistent  $Z$  values of the interface at different gate voltages, and revealed two superconducting gaps. The two gaps are associated with the two-band superconducting nature of few-layer NbSe<sub>2</sub> with a small interband scattering. We fitted the temperature dependence of the two gaps with the two-band BCS model and extracted the interband scattering strength and gap to  $T_c$  ratios, which revealed the weak to moderately strong coupling strength for few-layer NbSe<sub>2</sub> systems.

Financial support from the Research Grants Council of Hong Kong (Projects 16300717, 16302215, and SBI17SC16) and technical support of the Raith-HKUST Nanotechnology

Laboratory for the electron-beam lithography facility at MCPFF are hereby acknowledged. T.H. and N.W. would like to

acknowledge the intriguing discussions with K. T. Law and P. Sheng.

- 
- [1] K. S. Novoselov, A. K. Geim, S. V. Morozov, D. Jiang, Y. Zhang, S. V. Dubonos, I. V. Grigorieva, and A. A. Firsov, *Science* **306**, 666 (2004).
- [2] J. Rodrigo and S. Vieira, *Physica C (Amsterdam)* **404**, 306 (2004).
- [3] J. D. Fletcher, A. Carrington, P. Diener, P. Rodière, J.-P. Brison, R. Prozorov, T. Olheiser, and R. W. Giannetta, *Phys. Rev. Lett.* **98**, 057003 (2007).
- [4] C. L. Huang, J.-Y. Lin, Y. T. Chang, C. P. Sun, H. Y. Shen, C. C. Chou, H. Berger, T. K. Lee, and H. D. Yang, *Phys. Rev. B* **76**, 212504 (2007).
- [5] M. Zehetmayer and H. W. Weber, *Phys. Rev. B* **82**, 014524 (2010).
- [6] T. Yokoya, T. Kiss, A. Chainani, S. Shin, M. Nohara, and H. Takagi, *Science* **294**, 2518 (2001).
- [7] E. Boaknin, M. Tanatar, J. Paglione, D. Hawthorn, F. Ronning, R. Hill, M. Sutherland, L. Taillefer, J. Sonier, S. Hayden *et al.*, *Phys. Rev. Lett.* **90**, 117003 (2003).
- [8] M. S. El-Bana, D. Wolverson, S. Russo, G. Balakrishnan, D. M. Paul, and S. J. Bending, *Supercond. Sci. Technol.* **26**, 125020 (2013).
- [9] N. E. Staley, J. Wu, P. Eklund, Y. Liu, L. Li, and Z. Xu, *Phys. Rev. B* **80**, 184505 (2009).
- [10] X. Xi, Z. Wang, W. Zhao, J.-H. Park, K. T. Law, H. Berger, L. Forró, J. Shan, and K. F. Mak, *Nat. Phys.* **12**, 139 (2015).
- [11] J. Lu, O. Zheliuk, I. Leermakers, N. F. Yuan, U. Zeitler, K. T. Law, and J. Ye, *Science* **350**, 1353 (2015).
- [12] Y. Saito, Y. Nakamura, M. S. Bahramy, Y. Kohama, J. Ye, Y. Kasahara, Y. Nakagawa, M. Onga, M. Tokunaga, T. Nojima, Y. Yanase, and Y. Iwasa, *Nat. Phys.* **12**, 144 (2016).
- [13] B. T. Zhou, N. F. Q. Yuan, H.-L. Jiang, and K. T. Law, *Phys. Rev. B* **93**, 180501(R) (2016).
- [14] N. F. Q. Yuan, B. T. Zhou, W.-Y. He, and K. Law, *AAPPS Bull.* **26**, 12 (2016).
- [15] W.-Y. He, B. T. Zhou, J. J. He, N. F. Q. Yuan, T. Zhang, and K. Law, [arXiv:1604.02867](https://arxiv.org/abs/1604.02867).
- [16] D. Efetov, L. Wang, C. Handschin, K. Efetov, J. Shuang, R. Cava, T. Taniguchi, K. Watanabe, J. Hone, C. Dean *et al.*, *Nat. Phys.* **12**, 328 (2015).
- [17] M. R. Sahu, P. Raychaudhuri, and A. Das, *Phys. Rev. B* **94**, 235451 (2016).
- [18] C. W. J. Beenakker, *Phys. Rev. Lett.* **97**, 067007 (2006).
- [19] D. K. Efetov and K. B. Efetov, *Phys. Rev. B* **94**, 075403 (2016).
- [20] G. E. Blonder, M. Tinkham, and T. M. Klapwijk, *Phys. Rev. B* **25**, 4515 (1982).
- [21] L. Wang, I. Meric, P. Huang, Q. Gao, Y. Gao, H. Tran, T. Taniguchi, K. Watanabe, L. Campos, D. Muller *et al.*, *Science* **342**, 614 (2013).
- [22] See Supplemental Material at <http://link.aps.org/supplemental/10.1103/PhysRevB.97.060505> for the extraction of bias voltage on the interface of the heterojunction.
- [23] I. Giaever, *Phys. Rev. Lett.* **5**, 464 (1960).
- [24] J. R. Schrieffer, *Theory of Superconductivity* (Perseus Books, New York, 1999).
- [25] A. F. Andreev, *Sov. Phys. JETP* **19**, 1228 (1964).
- [26] K. Novoselov, A. K. Geim, S. Morozov, D. Jiang, M. Katsnelson, I. Grigorieva, S. Dubonos, and A. Firsov, *Nature (London)* **438**, 197 (2005).
- [27] J. Linder and A. Sudbø, *Phys. Rev. B* **77**, 064507 (2008).
- [28] J. Bardeen, L. N. Cooper, and J. R. Schrieffer, *Phys. Rev.* **108**, 1175 (1957).
- [29] H. Suhl, B. Matthias, and L. Walker, *Phys. Rev. Lett.* **3**, 552 (1959).
- [30] A. Brinkman, A. A. Golubov, H. Rogalla, O. V. Dolgov, J. Kortus, Y. Kong, O. Jepsen, and O. K. Andersen, *Phys. Rev. B* **65**, 180517(R) (2002).